Extended State Observer with Phase Compensation to Deal with High-frequency Vibrations in Hard Disk Drives

Minghui Zheng, Xu Chen, and Masayoshi Tomizuka

(CML Report 2015)

Mechanical Engineering

University of California, Berkeley

December 2015

Abstract

The extended state observer, as a special case of the high-gain observer, can estimate not only the state variables but also the unknown disturbances. Such estimation works well for slowly time-varying/low-frequency disturbances. To extend its performance to high-frequency disturbance estimation, this report introduces a phase compensator to recover the inherent phase loss in regular observers, and nonlinear gains to deal with the 'peak phenomenon' in traditional linear high-gain observers. By combining the nonlinear extended state observer with phase compensation and frequency-shaped sliding mode control, high-frequency vibrations can be suppressed effectively. Simulation on a hard disk drive demonstrates the efficiency of the proposed algorithm.

This work has been submitted to the 2016 American Control Conference (ACC) July, Boston, MA, USA

Contents

List of Figures

1 Introduction

In hard disk drives (HDDs), the specification for positioning accuracy becomes more stringent as the density of data storage becomes higher. Furthermore, mobile media opens a new market for HDDs while introducing higher requirements for both accuracy and robustness of control, especially when there are large external high-frequency disturbances. They may excite high frequency resonances of HDDs and seriously affect the servo performance during both the track-seeking and the track-following processes. Therefore, it is of fundamental importance to attenuate the influence of such high-frequency vibrations.

The extended state observer (ESO) is a promising method to estimate and suppress the disturbances. It treats the disturbances as state variables, and design state observers to estimate the disturbances. ESO is proposed by Han (2009), generalized and implemented in discrete time by Miklosovic et al. (2006). The effectiveness of ESO for a large class of disturbances was demonstrated by simulation and experiments Wang and Gao (2003); Radke and Gao (2006); Yang and Huang (2009); Zheng et al. (2012). By utilizing the robustness of high gains for disturbances, ESO has several good properties. It can deal with not only linear time-invariant systems, but also time-varying and nonlinear systems. It does not require an accurate plant or the inverse of the plant. An ESO can deal with a large class of disturbances without changing the structure and parameters, and provide good disturbance estimation both in time and frequency domains. Because of such properties, ESO has been applied to many areas and combined with other controllers Zheng and Gao (2010).

Existing ESO performs well for slowly time-varying disturbances; however, such property is not obvious for fast time-varying/high frequency disturbances. The main reason for this is the phase delay introduced by both the plant and ESO itself. For low-frequency disturbances, the effect of a small delay can be trivial. However, in HDDs, the disturbances usually include large high-frequency components, and a small delay may cause large estimation error. Motivated by such obstacles, this report extends the ESO's performance range from low frequencies to high frequencies. Specifically, a compensation filter is designed to compensate the phase delay. Moreover, nonlinear gains are designed instead of linear gains in ESO to reduce the 'peak phenomenon' in linear high gain observers Khalil and Praly (2014). The proposed compensated nonlinear ESO is combined with a frequency-shaped sliding mode control (SMC) to suppress high-frequency vibrations in HDDs.

The remainder of the report is organized as follows. Section II introduces the standard ESO. Section III designs a phase compensator and nonlinear gains for the ESO. Section IV combines the ESO with a frequency-shaped SMC algorithm. Section V demonstrates the benefits through simulation. Section VI concludes the report.

2 Standard Extended State Observer

2.1 Augmented System

Consider a general linear system describe by

$$\begin{aligned} \dot{x} &= Ax + B(u + d) \\ y &= Cx \end{aligned} \tag{2.1}$$

where $x \in \Re^{n\times 1}$ is the state vector; $y \in \Re$ is the output; $u \in \Re$ is the control input; $d \in \Re$ is the unknown disturbance; $A \in \Re^{n\times n}$; $B \in \Re^{n\times 1}$; and $C \in \Re^{1\times n}$. Assume that (C, A) is observable, d and its derivative $\dot{d}$ are bounded by δ_d and δ_d', respectively.

By treating d as a state variable, and $\dot{d}$ as the unknown disturbance, the system is rewritten as

$$\begin{aligned} \begin{bmatrix} \dot{x} \\ \dot{d} \end{bmatrix} &= \begin{bmatrix} A & B \\ 0 & 0 \end{bmatrix} \begin{bmatrix} x \\ d \end{bmatrix} + \begin{bmatrix} B \\ 0 \end{bmatrix} u + \begin{bmatrix} 0 \\ 1 \end{bmatrix} \dot{d} \\ y &= \begin{bmatrix} C & 0 \end{bmatrix} \begin{bmatrix} x \\ d \end{bmatrix} \end{aligned} \tag{2.2}$$

Denote

$$\begin{aligned} A_e &= \begin{bmatrix} A & B \\ 0 & 0 \end{bmatrix}, B_e = \begin{bmatrix} B \\ 0 \end{bmatrix}, B_d = \begin{bmatrix} 0 \\ 1 \end{bmatrix} \\ C_e &= \begin{bmatrix} C & 0 \end{bmatrix}, x_e = \begin{bmatrix} x^T & d^T \end{bmatrix}^T \end{aligned}$$

Then

$$\begin{aligned} \dot{x}_e &= A_e x_e + B_e u + B_d \dot{d} \\ y &= C_e x_e \end{aligned} \tag{2.3}$$

An state observer can be designed for the augmented system of Eq. (2.3) to estimate both the disturbance d and the states x.

2.2 Observability Analysis

Before designing the observer for the system described by Eq. (2.3), the observability needs to be analyzed. This section provides the necessary and sufficient condition for the observability of system (2.2).

Define the following function

$$Q(\lambda; A, C) = \begin{bmatrix} A - \lambda I \\ C \end{bmatrix} \tag{2.4}$$

where I is an identity matrix with compatible dimension.

Theorem (PBH Test) Hautus (1969) System of Eq. (2.1) is observable if and only if $Q(\lambda; A, C)$ has rank n for all $\lambda \in \mathbb{C}$.

Base on this, we have the following proposition.

Proposition: The system in Eq. (2.2) is observable if and only if the following two conditions hold:
(a) $(C,\ A)$ is observable;
(b) rank$\{Q(0; A_e, C_e)\}= n + 1$, where

$$Q(0; A_e, C_e) = \begin{bmatrix} A & B \\ 0 & 0 \\ C & 0 \end{bmatrix} \tag{2.5}$$

(i) Sufficiency proof: we first prove that (a) and (b) imply the observability of system (2.2). Given any $\lambda \in \mathbb{C}$, the following two cases are considered. (1) If $\lambda \neq 0$: the observability of $(C,\ A)$ implies that rank $\{Q(\lambda; A, C)\} = n$, which further implies that rank $\{Q(\lambda; A_e, C_e\} = n + 1$. (2) If $\lambda = 0$: rank$\{Q(0; A_e, C_e)\}= n + 1$. Therefore, $\forall \lambda \in \mathbb{C}$, rank$\{Q(\lambda; A_e, C_e)\}= n + 1$, which implies that (C_e, A_e) is observable.
(ii) Necessary proof: we now prove that the observability of system (2.2) implies (a) and (b). (1) The observability of (C_e, A_e) obviously implies the observability of (C, A). (2) The observability of (C_e, A_e) implies that rank$\{Q(\lambda; A_e, C_e)\}= n + 1$ $(\forall \lambda \in \mathbb{C})$, which further implies that rank$\{Q(0; A_e, C_e\}= n + 1$ by setting $\lambda = 0$. Therefore, the observability of augmented system (2.2) implies conditions (a) and (b).

Many systems can satisfy conditions (a) and (b), such as

$$A = \begin{bmatrix} -a_{n-1} & 1 & 0 & \cdots & 0 \\ -a_{n-2} & 0 & 1 & \cdots & 0 \\ \vdots & \vdots & \vdots & \vdots & \vdots \\ -a_0 & 0 & 0 & 0 & 0 \end{bmatrix}, B = \begin{bmatrix} b_{n-1} \\ b_{n-2} \\ \vdots \\ b_0 \end{bmatrix},$$
$$C = \begin{bmatrix} 1 & 0 & 0 & \cdots & 0 \end{bmatrix}$$

As long as $b_0 \neq 0$, conditions (a) and (b) are satisfied.

2.3 Standard Extended State Observer

The standard extended state observer (ESO) for System (2.1) is designed as follows, which is actually a standard state observer for System (2.2),

$$\begin{aligned}\begin{bmatrix}\dot{\hat{x}}\\ \dot{\hat{d}}\end{bmatrix} &= \begin{bmatrix}A & B\\ 0 & 0\end{bmatrix}\begin{bmatrix}\hat{x}\\ \hat{d}\end{bmatrix} + \begin{bmatrix}B\\ 0\end{bmatrix}u + \\ &\qquad \begin{bmatrix}L_x\\ L_d\end{bmatrix}\left(\begin{bmatrix}C & 0\end{bmatrix}\begin{bmatrix}x\\ d\end{bmatrix} - \begin{bmatrix}C & 0\end{bmatrix}\begin{bmatrix}\hat{x}\\ \hat{d}\end{bmatrix}\right)\end{aligned} \tag{2.6}$$

where $L_x = [\beta_1\ \beta_2\ ...\ \beta_n]^T$ and $L_d = \beta_{n+1}$. From Eqs. (2.2) and (2.6),

$$\begin{aligned}\begin{bmatrix}\dot{e}_x\\ \dot{e}_d\end{bmatrix} &= \begin{bmatrix}A - L_xC & B\\ -L_dC & 0\end{bmatrix}\begin{bmatrix}e_x\\ e_d\end{bmatrix} + B_d\dot{d}\\ e_d &= C_d\begin{bmatrix}e_x & e_d\end{bmatrix}^T\end{aligned} \tag{2.7}$$

where $e_x = x - \hat{x}$ is the state estimation error; $e_d = d - \hat{d}$ is the disturbance estimation error; and $C_d = [0 \quad 1]$. e_x and e_d are preferred to be as small as possible in the presence of unknown $\dot{d}$.

During the design of the observer in Eq. (2.6), $\dot{d}$ is actually assumed as zero, i.e., $\dot{d} = 0$. This explains why the standard ESO is effective for slow time-varying disturbances and low-frequency vibrations.

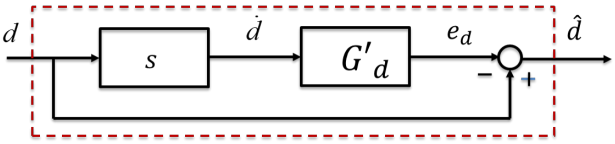

Figure 1: Dynamic System from d to $\hat{d}$

Let $G_d^{'}$ denote the transfer function from $\dot{d}$ to e_d. From Eq. (2.7), we have

$$\begin{aligned}G_d^{'} &= C_d(sI - \begin{bmatrix}A - L_xC & B\\ -L_dC & 0\end{bmatrix})^{-1}B_d\\ &= (s + L_dC(sI_x - A + L_xC)^{-1}B)^{-1}\end{aligned} \tag{2.8}$$

Let G_d denote the transfer function from d to $\hat{d}$. The relationship among d, $\hat{d}$ and $\dot{d}$ is as shown in Fig.1. From Fig. 1, we have

$$\begin{aligned}G_d &= 1 - sG_d^{'}\\ &= 1 - s(s + L_dC(sI_x - A + L_xC)^{-1}B)^{-1}\end{aligned} \tag{2.9}$$

Denote $G_x = C(sI_x - A + L_xC)^{-1}B$, then

$$G_d = 1 - s(s + L_dG_x)^{-1} = \frac{L_dG_x}{s + L_dG_x} \tag{2.10}$$

Ideally, $G_d = 1$. This ideal case can be approximated by choosing a large L_d. If $L_d \gg 1$ such that $\|L_d(jw)G_d(jw)\| \gg w$, we have $|G_d(j\omega)| \approx 1$ and $\angle G_d(j\omega) \approx 0°$. This explains why the high gain (L_d) is required for ESO. In practice, G_d proximately performs as a low-pass filter whose bandwidth depends on L_d. To ensure accurate state estimation, L_x should also be large enough to reduce the effect of unknown $\dot{d}$. Usually we select $L_d > L_{x,n} > L_{x,n-1} > ... > L_{x,1}$ (i.e., $\beta_{n+1} > \beta_n > ... > \beta_1$).

3 Phase Compensation in Nonlinear Extended State Observer

3.1 Phase Compensation

This section extends the performance range of the standard ESO from low frequencies to high frequencies based on the assumption that the majority of the disturbance's power focuses on high frequencies, for example, around ω_0 Hz. Fig.2 provides the frequency response of the transfer function from the actual disturbance to its estimate. It is noticed that at low frequencies, the magnitude of G_d is approximately 1 and the phase of G_d is approximately 0, and the disturbance estimation is good. As the frequency increases, phase delay becomes larger, which would seriously degrade the accuracy of the estimation. In this case, a phase compensator G_c needs to be introduced to the standard ESO, which results in a compensated ESO.

Let $\hat{d}_c$ denote the estimated disturbance from the compensated ESO. Let G_{dc} denote the transfer function from d to $\hat{d}_c$, i.e.,

$$\hat{d}_c = G_{dc}d = \frac{L_dG_xG_c}{s + L_dG_x}d \tag{3.1}$$

G_{dc} is desired to have zero phase at ω_0. With this goal, G_c is designed as

$$G_c = \frac{s + \omega_0/\alpha}{s + \alpha\omega_0} \ (\alpha > 1) \tag{3.2}$$

Based on Eq. (3.2), the phase compensated at ω_0 is

$$\varphi_m = \arcsin\frac{\alpha^2 - 1}{\alpha^2 + 1} \tag{3.3}$$

where α is designed such that $\angle G_{dc}(\omega_0) = 0$, as shown in Fig. 2. G_c can be realized by

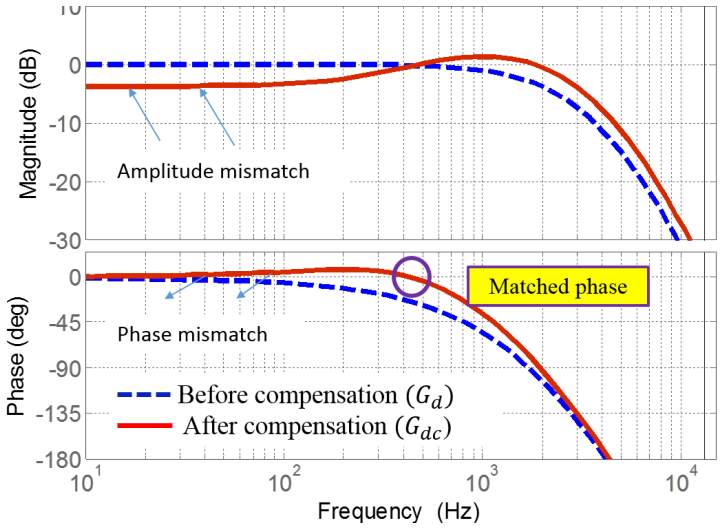

Figure 2: Frequency Responses of G_d and G_{dc}

the following system:

$$\begin{aligned} \dot{\hat{z}} &= A_c\hat{z} + B_c\hat{d} \\ \hat{d}_c &= C_c\hat{z} + D_c\hat{d} \end{aligned} \tag{3.4}$$

where $A_c = -\alpha\omega_0$, $B_c = \omega_0/\alpha - \alpha\omega_0$, $C_c = 1$, $D_c = 1$. From Equations (2.6) and (3.4), the compensated ESO becomes:

$$\begin{aligned} \begin{bmatrix} \dot{\hat{x}} \\ \dot{\hat{z}} \\ \dot{\hat{d}} \end{bmatrix} &= \begin{bmatrix} A & 0 & B \\ 0 & A_c & B_c \\ 0 & 0 & 0 \end{bmatrix} \begin{bmatrix} \hat{x} \\ \hat{z} \\ \hat{d} \end{bmatrix} + \begin{bmatrix} B \\ 0 \\ 0 \end{bmatrix} u + \begin{bmatrix} L_x(y - C\hat{x}) \\ 0 \\ L_d(y - C\hat{x}) \end{bmatrix} \\ \begin{bmatrix} \hat{x} \\ \hat{d}_c \end{bmatrix} &= \begin{bmatrix} I & 0 & 0 \\ 0 & C_c & D_c \end{bmatrix} \begin{bmatrix} \hat{x} \\ \hat{z} \\ \hat{d} \end{bmatrix} \end{aligned} \tag{3.5}$$

3.2 Nonlinear Extended State Observer

As explained in Section II, the ESO belongs to the class of high-gain observers. If the initial estimation error is large, such high gains may cause the 'peak phenomenon' and make the linear ESO impractical or even unsafe to use Khalil (2008); Khalil and Praly (2014). Nonlinear gains are usually utilized to reduce such peak phenomenon. A nonlinear function is proposed as follows in Han (2009), based on which nonlinear gains can be

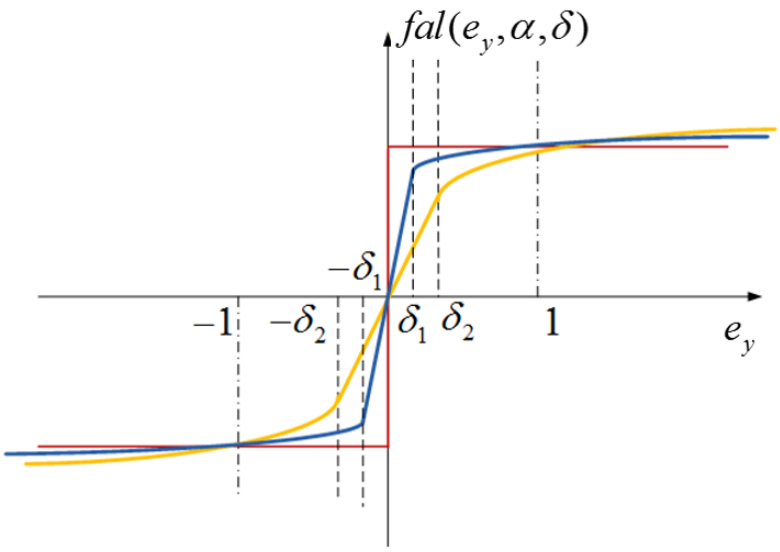

Figure 3: Nonlinear Functions in Nonlinear ESO

designed,

$$fal(e_y) = \begin{cases} \frac{e_y}{\delta^{1-\alpha}}, & |e_y| \le \delta \\ |e_y|^{\alpha}\text{sign}(e_y), & |e_y| \ge \delta \end{cases} \tag{3.6}$$

where δ and α are design parameters; $e_y = y - C\hat{x}$. Figure 3 illustrates this nonlinear function. The following nonlinear gains for the ESO based on Eq. (3.6) are designed as

$$\begin{cases} f_x(e_y) = L_{x,i}\delta^{1-\alpha} fal(e_y) + K_{x,i}e_y, \ i = 1, ..., n \\ f_d(e_y) = L_d\delta^{1-\alpha} fal(e_y) + K_d e_y \end{cases} \tag{3.7}$$

where $K_{x,i}$ and K_d are small. A nonlinear extended state observer based on Eq. (3.5) is proposed as

$$\begin{aligned} \begin{bmatrix} \dot{\hat{x}} \\ \dot{\hat{z}} \\ \dot{\hat{d}} \end{bmatrix} &= \begin{bmatrix} A & 0 & B \\ 0 & A_c & B_c \\ 0 & 0 & 0 \end{bmatrix} \begin{bmatrix} \hat{x} \\ \hat{z} \\ \hat{d} \end{bmatrix} + \begin{bmatrix} B \\ 0 \\ 0 \end{bmatrix} u + \begin{bmatrix} f_x(e_y) \\ 0 \\ f_d(e_y) \end{bmatrix} \\ \begin{bmatrix} \hat{x} \\ \hat{d}_c \end{bmatrix} &= \begin{bmatrix} I & 0 & 0 \\ 0 & C_c & D_c \end{bmatrix} \begin{bmatrix} \hat{x} \\ \hat{z} \\ \hat{d} \end{bmatrix} \end{aligned} \tag{3.8}$$

When the error is small ($|e_y| \leq \delta$), high gains are implemented to obtain the robustness to unknown dynamics and disturbances. When the error is large ($|e_y| > \delta$), high gains are saturated to reduce large transient behaviors.

4 Frequency-shaped Sliding Mode Control

This section describes the controller design process. A frequency-shaped sliding mode control (FSSMC) algorithm Zheng et al. (2014) based on the nonlinear compensated ESO is introduced. The control system is shown in Fig.4.

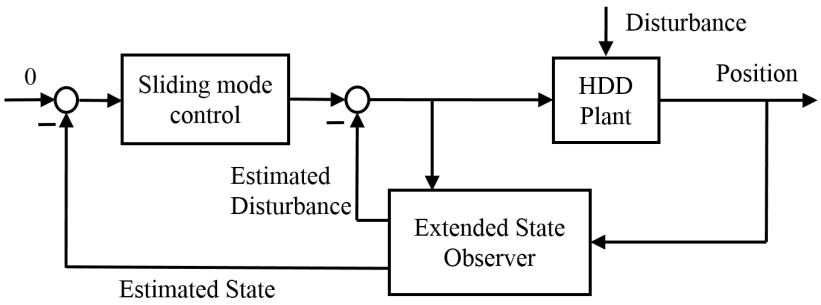

Figure 4: System Structure

With the ESO designed in Eq. (3.8), noting $e_{dc} = d - \hat{d}_c$, Eq. (2.1) becomes

$$\begin{aligned} \dot{x} &= Ax + B(u + \hat{d}_c + e_{dc}) \\ y &= Cx \end{aligned} \tag{4.1}$$

Denote $\bar{u} = u + \hat{d}_c$, we have

$$\begin{aligned} \dot{x} &= Ax + B(\bar{u} + e_{dc}) \\ y &= Cx \end{aligned} \tag{4.2}$$

The frequency-shaped sliding mode control (FSSMC) algorithm provides further enhancement at the frequencies where the servo performance is seriously degraded by large disturbances such as audio vibrations Zheng et al. (2014). Specifically, a peak filter Q_f is introduced to shape the sliding surface at the preferred frequencies. In this report, Q_f is designed as a peak filter,

$$Q_f(p) = \frac{B(p)}{A(p)} = \frac{p^2 + 2bw_d p + w_d^2}{p^2 + 2aw_d p + w_d^2} \tag{4.3}$$

where $0 < a < b < 1$, p is the Laplace variable and w_d is the peak frequency.

For system (4.2), in traditional SMC, the sliding variable s is usually defined as

$$s = Hx = \begin{bmatrix} 1 & \lambda \end{bmatrix} \begin{bmatrix} x_1 \\ x_2 \end{bmatrix}$$

where $\lambda \in \Re^{1\times(n-1)}$, and $x_2 \in \Re^{(n-1)\times 1}$. In FSSMC, it is modified to

$$s = H \begin{bmatrix} Q_f\{x_1\} \\ x_2 \end{bmatrix} = x_{1f} + \lambda x_2 \tag{4.4}$$

where x_{1f} is the filtered error, i.e., $x_{1f} = Q_f\{x_1\}$. Assume that Q_f has the following state-space realization:

$$\begin{aligned} \dot{x}_w &= A_w x_w + B_w x_1 \\ x_{1f} &= C_w x_w + D_w x_1 \end{aligned} \tag{4.5}$$

Combining Eq. (4.1) and Eq. (4.5), the augmented system with Q_f is represented as

$$\begin{aligned} \begin{bmatrix} \dot{x} \\ \dot{x_w} \end{bmatrix} &= \begin{bmatrix} A & 0 \\ B_w C & Aw \end{bmatrix} \begin{bmatrix} x \\ x_w \end{bmatrix} + \begin{bmatrix} B \\ 0 \end{bmatrix} (u + \hat{d}_c + e_{dc}) \\ &\triangleq \bar{A} x_e + \bar{B}(u + \hat{d}_c + e_{dc}) \end{aligned} \tag{4.6}$$

From Eqs.(4.4) and (4.5), the sliding variable becomes

$$\begin{aligned} s &= x_{1f} + \lambda x_2 \\ &= C_w x_w + D_w x_1 + \lambda x_2 \\ &= [C_w \ D_w \ \lambda][x_w \ x_1 \ x_2]^T \triangleq \bar{H} x_e \end{aligned} \tag{4.7}$$

Then the FSSMC control law is proposed as

$$u = (\bar{H}\bar{B})^{-1}[-qs - \bar{H}\bar{A}x_e - \gamma \bar{H}\bar{B}\, sgn(s)] - \hat{d}_c \tag{4.8}$$

where $\gamma \geq |e_{dc}|$. Substituting Eq. (4.8) into Eq. (2.1), after some algebra, the following approaching dynamics of the system is obtained

$$\dot{s} = -qs - (\gamma - e_{dc})(\bar{H}\bar{B}) sgn(s) \tag{4.9}$$

Through the standard analysis in SMC, s would converge to zero. A boundary layer can be introduced to reduce chattering brought by the 'sign' function. Write the controller in Eq. (4.8) compactly as follows

$$u' = g(x, x_\omega, s(x, x_\omega)) - \hat{d}_c \tag{4.10}$$

When the state variables are not directly available, x can be replaced by $\hat{x}$ in Eq. (4.10),

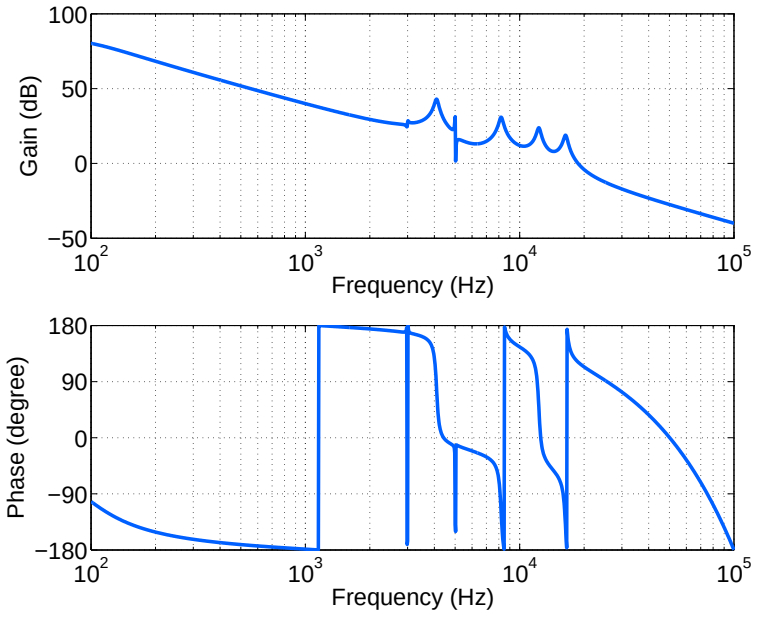

Figure 5: Full Order Model of HDD (IEEJ, 2007)

and the control law becomes

$$u = g(\hat{x}, \hat{x}_\omega, s(\hat{x}, \hat{x}_\omega)) - \hat{d}_c \tag{4.11}$$

where $\hat{x}_w$ is the state variables of the system in Eq. (4.5) with replacing x_1 by $\hat{x}_1$. The controller in Eq. (4.11) guarantees the stability of the system in Eq. (2.1) in the presence of d, with desired frequency properties and good estimation and suppression of the disturbance.

5 Simulation Results

The proposed control algorithm (the combination of the nonlinear extended state observer with phase combination and a frequency-shaped sliding mode controller) is implemented on the full-order benchmark plant IEEJ (2007) which can be approximately described by

$$G_{\text{hdd}}(p) = \frac{k_y k_v}{p^2} + \sum_{i=1}^{4} \left(\frac{{w_i}^2}{p^2 + 2\xi w_i p + {w_i}^2} \right) \tag{5.1}$$

The bode plot for the HDD plant is shown in Fig. 5. The plant parameters are as follows:

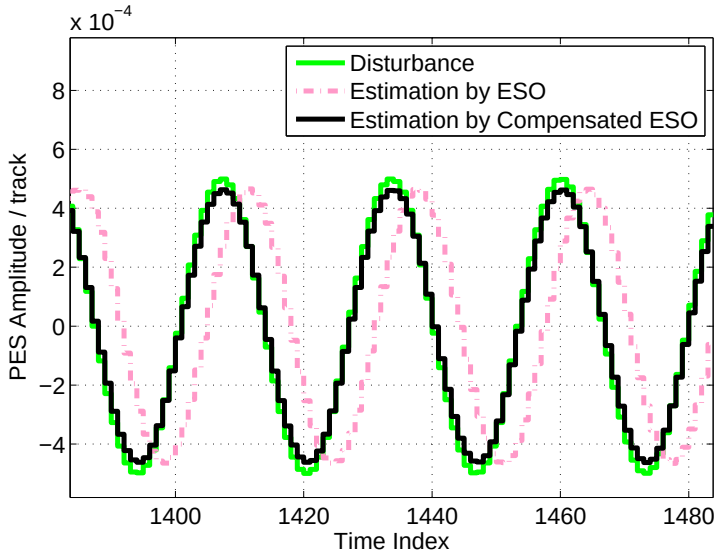

Figure 6: Disturbance Estimation by ESO (Single Tone)

the acceleration constant k_v=951.2 m/(s^{2}A); the position measurement gain k_y=3.937 $\times$ 10^6 track $\cdot$ m^{-1}; the four main resonance central frequencies w_i's ($i = 1, ..., 4$) are 4100 Hz, 8200 Hz, 12300 Hz, 16400 Hz, respectively; and the corresponding damping factor ξ is 0.02. In the following simulation, the gains of the extended state observers are nonlinear.

Figure 6 and Figure 7 compare the disturbance estimation between the ESO and the compensated ESO. The disturbance source in Figure 6 is a sinusoid signal with the frequency of 1000 Hz. It is observed that there is nearly no delay between the disturbance and its estimation by the compensated ESO, while the standard ESO estimates the disturbance with a phase delay. The disturbance source in Figure 7 is from actual experiments on HDDs in the presence of strong audios, whose majority power is around 1000 Hz. Similar to Figure 6, Figure 7 shows that the compensated ESO has better estimation of the disturbance than the standard ESO.

Figures 8 to 10 compare the PES spectrums among four different control systems: (a) standard SMC without ESO; (b) standard SMC with the standard ESO; (c) frequency-shaped SMC with the standard ESO; (d) frequency-shaped SMC with the compensated ESO. The accumulative 3σ value of PES is calculated and shown at the top right corn of each figure. As shown in Figure 8, comparing with system (a), the PES of system (b) below 500 Hz is reduced, which illustrates the effectiveness of ESO for low-frequency disturbance estimation. Figure 9 compares (b) and (c), and the PES around 1000 Hz is reduced by the frequency shaping technique in FSSMC. Figure 10 compares (c) and (d), and the PES around 500 Hz is reduced by the compensation filter in the compensated ESO. Overall,

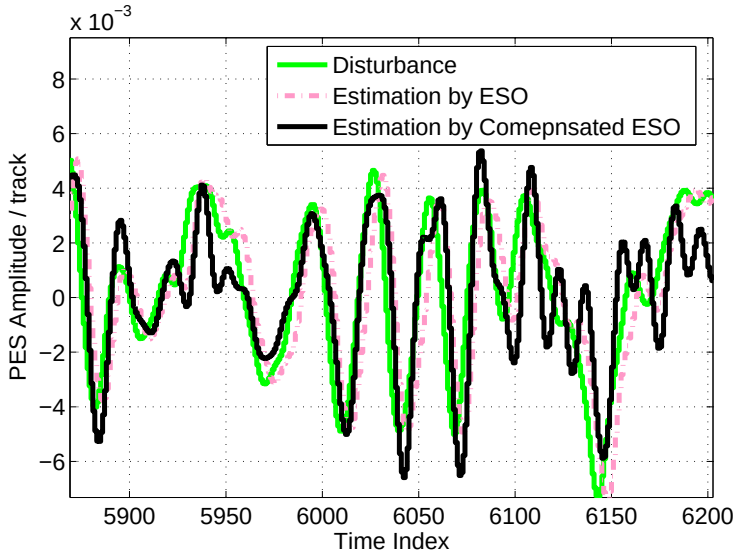

Figure 7: Disturbance Estimation by ESO (Audio-vibrations)

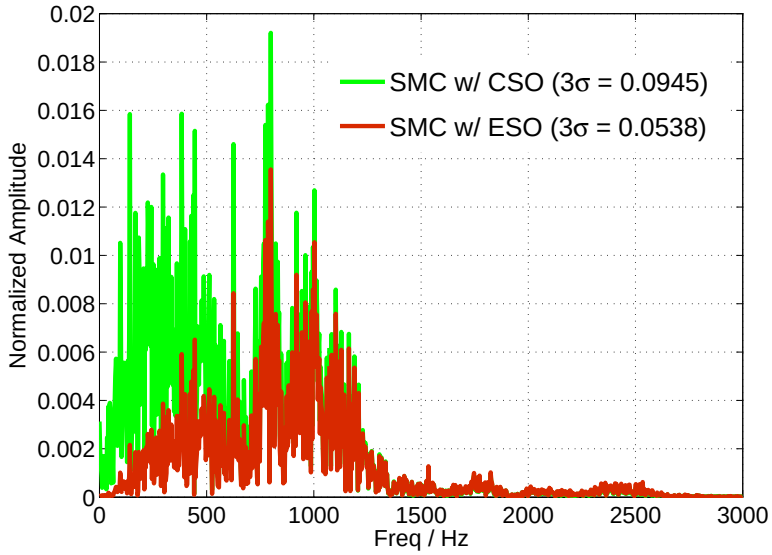

Figure 8: Vibration Rejection by ESO (Audio-vibrations)

the 3σ value of the PES has been reduced from 9.45% to 2.01%, with frequency shaping techniques in both the controller and the observer.

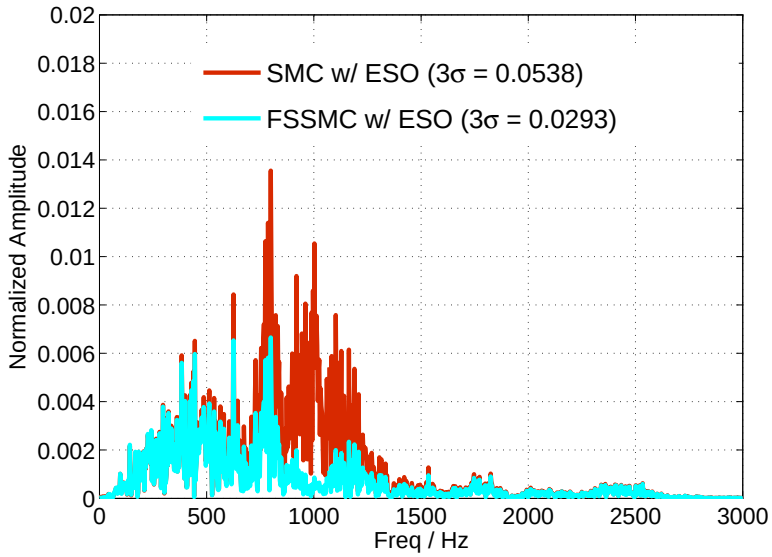

Figure 9: Vibration Rejection by FSSMC (Audio-vibrations)

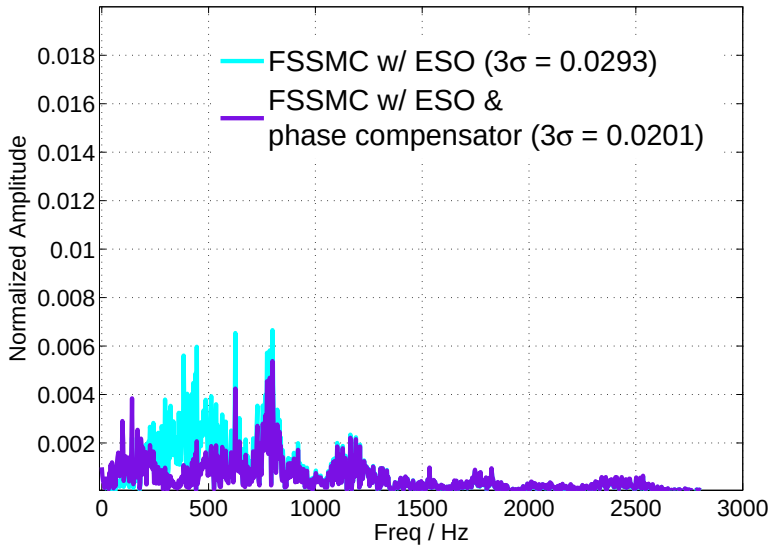

Figure 10: Vibration Rejection by ESO and FSSMC (Audio-vibrations)

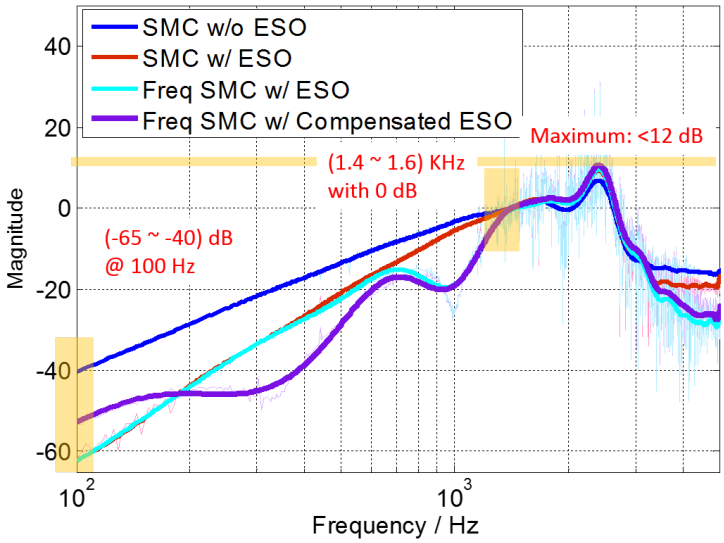

Figure 11: Measured and Fitted Sensitivities from Vibrations to PES

The sensitivity from the disturbances to the PES is a key criterion to evaluate the servo performance in HDDs. The systems discussed in this report are nonlinear, and there are no analytical solutions of the sensitivity functions for those systems. Instead, Figure 11 provides both the measured and the fitted frequency responses of the sensitivity functions in systems (a) to (d). It is shown that system (d) has better vibration suppression than systems (a) (b) and (c), with insignificant sacrifice at other frequencies.

6 Conclusion

The report proposed a phase compensator for the extended state observer. It compensated the phase delay which exists in the standard extended observer, and provided more accurate estimate for high-frequency disturbance. At the same time, nonlinear gains were designed for the compensated extended state observer to reduce the peak phenomenon and avoid large transient behaviors. A frequency-shaped sliding mode control algorithm was implemented with the compensated nonlinear ESO to further suppress large peaks in the vibrations. Simulation results validated the performance enhancement. Some future work may include adaptive extended state observer design when the peak frequencies of the disturbance is unknown.

References

Han, J. (2009). From PID to active disturbance rejection control. *Industrial Electronics, IEEE Transactions on*, 56(3):900–906.

Hautus, M. L. J. (1969). Controllability and observability condition of linear autonomous systems. *Ned. Akad. Wetenschappen, Proc. Ser. A,*, 72:445–455.

IEEJ (2007). IEEJ technical commitee for novel nanoscale servo control, nss benchmark problem of hard disk drive systems. *http://mizugaki.iis.u-tokyo.ac.jp/nss/*.

Khalil, H. (2008). High-gain observers in nonlinear feedback control. In *Control, Automation and Systems, 2008. ICCAS 2008. International Conference on*, pages xlvii–lvii.

Khalil, H. and Praly, L. (2014). High-gain observers in nonlinear feedback control. In *Int. J. Robust Nonlinear Control*, volume 24, page 9931015.

Miklosovic, R., Radke, A., and Gao, Z. (2006). Discrete implementation and generalization of the extended state observer. In *Procedings of the American Control Conference*, pages 2209–2214.

Radke, A. and Gao, Z. (2006). A survey of state and disturbance observers for practitioners. In *Procedings of the American Control Conference*, pages 5183–5188.

Wang, W. and Gao, Z. (2003). A comparison study of advanced state observer design techniques. In *American Control Conference, 2003. Proceedings of the 2003*, volume 6, pages 4754–4759 vol.6.

Yang, X. and Huang, Y. (2009). Capabilities of extended state observer for estimating uncertainties. In *Procedings of the American Control Conference*, pages 3700–3705.

Zheng, M., Chen, X., and Tomizuka, M. (2014). Discrete-time frequency-shaped sliding mode control for audio-vibration rejection in hard disk drives. *Proceedings of the 19th IFAC World Congress 2014, Cape Town, South Africa, August 24-29, 2014*, 19:6843–6848.

Zheng, Q., Gao, L., and Gao, Z. (2012). On validation of extended state observer through analysis and experimentation. *Journal of Dynamic Systems, Measurement, and Control*, 134:024505,1–5.

Zheng, Q. and Gao, Z. (2010). On practical applications of active disturbance rejection control. In *2010 29th Chinese Control Conference (CCC)*, pages 6095–6100.